

21



1530

COLLÈGE DE FRANCE
Laboratoire de Physique Corpusculaire

CERN LIBRARIES, GENEVA

CERN LIBRARIES, GENEVA



CM-P00063313

LPC 93 32 / Conf

STATUS REPORT ON THEMISTOCLE EXPERIMENT

THEMISTOCLE Collaboration

Presented by C. Ghesquière at the workshop
"Towards a major atmospheric Cerenkov detector for TeV astroparticle Physics"
Calgary, July 17 - 18, 1993

STATUS REPORT ON THEMISTOCLE EXPERIMENT

THEMISTOCLE Collaboration

P. Baillon², L. Behr³, S. Danagoulian^{3,*}, A. Djannati-Ataï¹, B. Dudelzak³, P. Espigat¹, P. Eschstruth³, B. Fabre⁶, G. Fontaine⁵, R. George⁴, C. Ghesquière¹, F. Kovacs⁴, C. Meynadier⁶, Y. Pons⁴, R. Riskalla³, M. Rivoal⁴, P. Roy³, P. Schune^{1,**}, A.M. Touchard⁴, J. Vrana⁵.

Abstract.

A brief account of the present set-up, the current performances and the sensitivity of the THEMISTOCLE Experiment is given. The emphasis is put on the points which have been developed in the last year, mainly on the energy estimation of the gamma showers.

A few developments under way to get a better rejection of the hadronic showers by using a crude imaging and a pulse shape analysis, are described.

Altogether we hope for an increase of 3 in the sensitivity.

Presented by C. Ghesquière at the workshop

"Towards a major atmospheric Cerenkov detector for TeV astroparticle Physics"
Calgary. July 17-18, 1993.

Keywords: Astrophysics, gamma astronomy, telescope counters, solar power plants

¹ Collège de France 11 Pl. M. Berthelot F-75231 Paris Cedex 05

² CERN CH-1211 Geneva 23

³ LAL Bat.200 Univ. Paris Sud F-91405 Orsay

⁴ LPNHE Univ. Paris 6-7 Tour 33 R.d.C. 4 Pl.Jussieu F-75252 Paris Cedex 05

⁵ LPNHE X Ecole Polytechnique F-91128 Palaiseau

⁶ Univ. de Perpignan Ave de Villeneuve F 66025 Perpignan Cedex

* Permanent adress: Yerevan Ph. Inst. Alikhanian Br. St. 2 Yerevan 375036 Armenia

** Now at DAPNIA CEN Saclay F-91191 Gif s. Yvette Cedex

Introduction.

The THEMISTOCLE Experiment had its set up completed by mid-90. Since then it has mainly observed the CRAB source in order to test the quality of the experiment, in three successive winter campaigns, the CRAB being in good observation (-35° to $+35^\circ$ from zenith) from October to March.

Only two sets of data from 90-91 and 91-92 have been fully analysed and are in the way to be published [1]. They correspond to a total of 76526 on-source and 56792 off-source events used for background evaluation.

Only the unpublished technical details and the evolution of the experiment will be described here.

Present lay-out.

Main characteristics of the apparatus.

- Site position : 42.50° N, 1.97° E, alt. 1650 m
- 18 stations scattered on a roughly elliptical field of axes respectively 280 and 190 m. Fig 1.

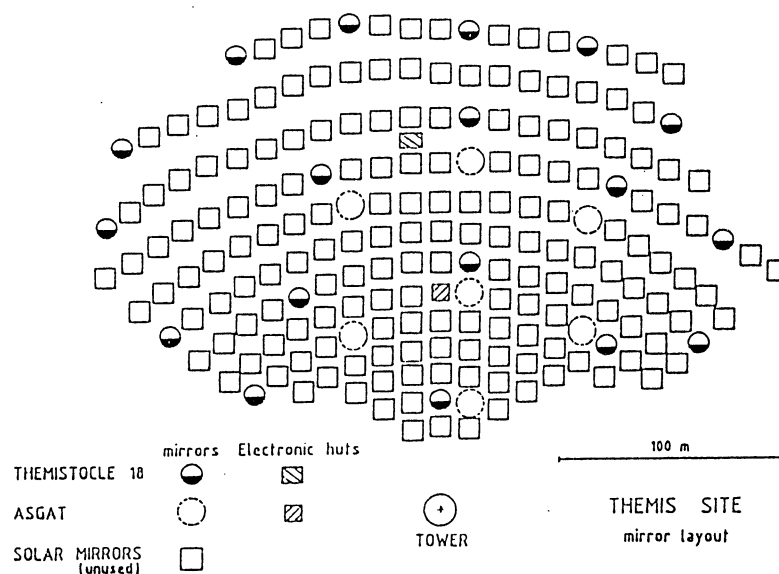


Fig 1: Lay out of the detectors

- Each station is equipped with a Cerenkov telescope:
 - Parabolic mirror 800 mm \varnothing (Effective area 0.465 m^2)
 - focal length 404 mm
 - Focal spot size 2 mr FWHM
 - Front face aluminisation + SiO_2 coating
 - Reflectivity 0.92 in the range 300-700 nm
- Single PM RTC XP2020- S11 photo cathode
- Rise time 1.8 ns at 10^7 gain
- Used gain $\approx 5 \cdot 10^5 + x \cdot 10$ preamp. (140 MHz B.W.)

Charge resolution 60% on single photo-electron.
Diaphragm full aperture 40 mr (No sharp edges due to aberrations of the large aperture optics)

- Trigger :

Individual PM threshold ≈ 9 ph.el. $\approx 4 \sigma$ from night sky background.

Majority coincidence $>10/18$ further reduced by software cut at $>12/18$.

Trigger rate 0.20 Hz for 10/18, 0.095 Hz for 12/18.

Angular accuracy.

A six parameter fit to the conical shape of the wave front needs 12 PM hits for a sufficient accuracy, hence there are not enough stations to estimate the accuracy by splitting the field into two independent sets. The overall resolution is given by the width of the Crab signal, assuming no prejudice from the natural width of the source.

The angular resolution is a linear function of the individual timing accuracy. The time of arrival of the wave front is measured to 0.1 ns precision after a CFD situated close to the PM.

The accuracy of the individual time measurements is well represented by the formula

$$\sigma_t = \sqrt{a^2 + \frac{b^2}{N_{\text{ph.el.}}}}$$

a and b vary slightly from PM to PM around the average values

$$a = 0.17 \text{ ns}$$

$$b = 2.7 \text{ ns}$$

The overall residuals after cone fitting are shown in Fig 2.

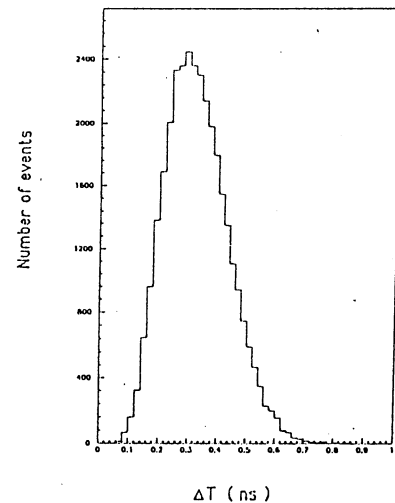


Fig 2. Residuals to the ideal cone after fit

The Crab signal is fitted to a two dimensional gaussian centered on the average direction, thus giving the miss to the theoretical source direction.

The result in angular accuracy is

$$\sigma_\theta = 2.3 \pm 0.3 \text{ mr (} 0.14^\circ \text{)}$$

slightly decreasing to 2.0 mr for the highest energies.

The source pointing accuracy is 0.50 mr (0.03°)

The sensitivity of the experiment can be evaluated with respect to the Crab integral flux, Φ , over 3 TeV

$$n_\sigma = 0.5 \sqrt{\frac{\Phi}{\Phi_{\text{cr}}} t} \quad t \text{ in hours} \quad (6.5 \sigma \text{ in } 120 \text{ h on CRAB})$$

Energy measurement.

Most of the recent work has been devoted to the energy estimation. The Cerenkov light is sampled by the telescopes involved in the trigger, 12 to 18, which are read by ADC's at a precision 0.3 ph-el/ADC channel.

The energy evaluation is based to a comparison between the data and simulated gamma showers by the CERN program : SIMDEL. This program is full M.C., including the earth magnetic field, the air absorption, the photo-cathode yield as a function of the wavelength, the optical aberrations and the PM and electronics response time.

The radial distribution of the Cerenkov light density was obtained at five fixed energies : 1, 3, 10, 30 and 100 TeV and average curves deduced for each energy. Fig 3.

Those distributions are smoothed by second order polynomials and interpolation between the coefficients of the polynomials allows to predict the radial distribution at each energy. The dispersion of the individual showers around those average curves are not Poisson like and taking as the variance of the measured points the square root of the theoretical value is an approximation which may lead to bad evaluation of the energy or some rejection of the showers.

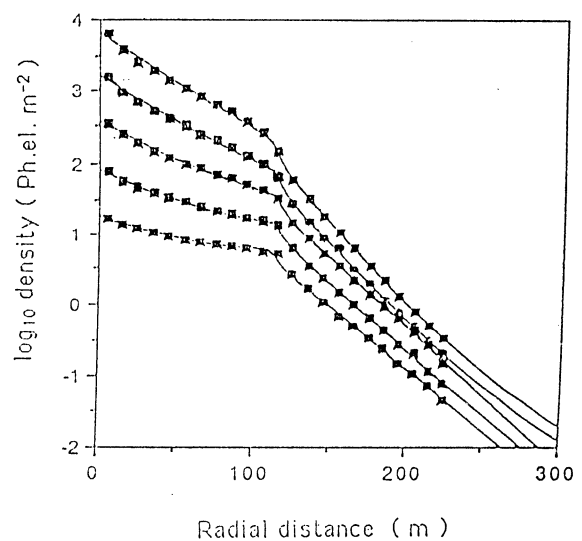


Fig 3. Average radial density distributions
Gamma rays of 1, 3, 10, 30, 100 TeV

Absolute calibration of energy.

Whatever care is taken in evaluating all yields and absorptions there remains a suspicion about the effective rate of transformation of a Cerenkov photon in a detected photon in terms of charge in the ADC's.

In order to check the validity of the simulation and to estimate rightly the energy, there is an overall scaling factor to be adjusted.

This factor is obtained using Monte Carlo hadronic showers generated according to the known flux of cosmic rays, processed through the detector and adjusted in energy in such a way as to reproduce the raw experimental trigger rate of off-source events. This in fact, amounts to move the hadron threshold, the trigger rate being a sharp function of the threshold :

$$\text{Tr. rate} \approx (E_{\text{threshold}})^{1.7}$$

Two other distributions of triggered off-source events are used to check the validity of the simulation : The distribution of trigger

multiplicity, Fig.4 and the sum of the ADC's per event : Fig. 5. The agreement between the simulated and the real events is quite good.

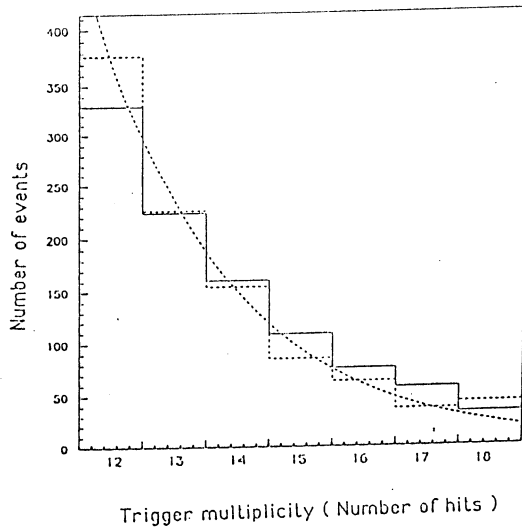


Fig. 4 .Trigger multiplicity
Full line : real events
Dotted line : Monte Carlo

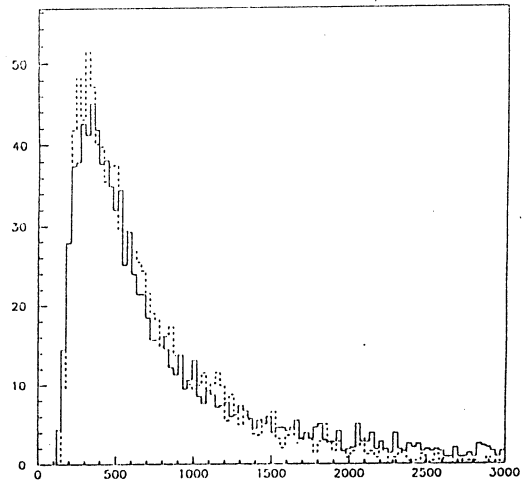


Fig. 5 .Sum of ADC per event
Full line : real events
Dotted line : Monte Carlo

Systematic errors.

There may be two causes to the systematic errors on the energy. The first is that the two distributions in Fig. 4 and 5 do not match exactly, the second comes from the uncertainties in the pN and NN interaction models. Comparing the results of three different models, discrepancies in the yield of production of Cerenkov light have shown up at the level of 20%.

We then conclude that a systematic uncertainty of order 20% is unavoidable in the present state of the art.

Energy reconstruction.

Several methods have been attempted to evaluate the energy on an event by event basis. Those methods are calibrated using M.C. generated gammas according to a differential spectrum in $E^{-2.4}$, each event being sent 11 times at a random position on the field and, if triggered, reconstructed and processed through the energy restitution with the reconstructed values for the parameters. The reconstructed energy can then be directly compared to the initial one.

As a general rule, when looking at the radial distributions we observe that most of the dispersion from shower to shower takes place near the core ($R < 20m$) or at large distance ($R > 130m$). For that reason in the process of energy reconstruction we retained only those telescopes which lay between 20 and 130 m from the reconstructed apex.

Within these limits several method were tried :

- a) Total sum of ADC's = $\sum ADC$

b) Reduced sum of ADC's $= \frac{1}{N} \sum_1^N \text{ADC}$. N is the number of telescopes hit in the interval.

c) Value of ADC at 75 m, interpolated from the flanking hits.

d) Min χ^2 between the hits and the radial density distribution:

$$\frac{\partial \chi^2}{\partial E} = 0, \chi^2 = \sum_{r_i=20}^{r_i=130} \frac{(D_{th}(E, r_i) - D_i(r_i))^2}{D_{th}(E, r_i)}$$

In the first try the fit is done using all the points contained in the interval $20 < R < 130$ m. The first value of the reduced χ^2 is called the "hadronicity"

$$h = \frac{1}{N-1} \sum_1^N \frac{(D_{th}(E, r_i) - D(r_i))^2}{D_{th}(E, r_i)}$$

We then proceed through two new iterative steps, each time removing the PM with the worst relative residual value :

$$\left| \frac{D_{th}(E, r_j) - D(r_j)}{(D_{th}(E, r_j))^{\frac{1}{2}}} \right|$$

After the removal of these two PM's the final value of the fitted energy is taken as the reconstructed energy value and the error on the energy obtained from the mean residual.

$$\frac{\Delta E}{E} = \frac{1}{N-3} \frac{\sqrt{\sum_1^{N-2} (D_{th}(E, r_i) - D_i(r_i))^2}}{\sum_1^{N-2} D_{th}(E, r_i)}$$

e) A last method consist to minimize the χ^2 to the radial distribution as in d), but weighting each point by a decreasing function, W_i , of the distance of the measured point to $r=75$ m, taken as the most stable point of the distributions:

$$W_i(r_i) = \frac{1}{1 + a(r_i - 75)^2}$$

From all these methods, d) gives the more information and the best gaussian distribution, on Fig 6a, of the quantity :

$$\frac{E_0 - E_{reconstructed}}{E_0}$$

The s.d. of the fitted gaussian $\sigma = 0.15$, gives a good idea of the accuracy of the reconstructed energy.

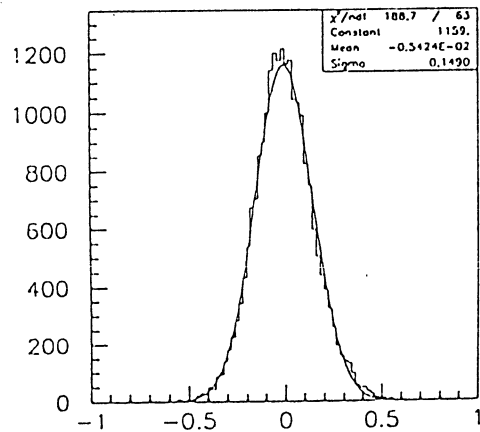


Fig. 6. Plot of $(E_{th} - E_{reconstructed}) / E_{th}$

using method d). See text

Moreover to take into account the variable attenuation, mostly dependent of the atmosphere variation, we applied to the reconstructed energy a scaling factor evaluated from the instant trigger rate compared to the average trigger rate (0.095 Hz) used to calculate the reference distributions :

$$E_{\text{final}} = E_{\text{Reconstructed}} \left(\frac{0.095}{\text{Trig. rate}} \right)^{\frac{1}{1.7}}$$

In Fig 7, the distribution of $\Delta E/E$ is shown as a function of the reconstructed energy. It goes from a mean value of 15% at the threshold of 3 TeV, to 12% at 20 TeV and over. In practice the tails near threshold are further cut by χ^2 conditions.

In real events, some effects which have not been implemented in the Monte Carlo, f.i. the uncorrected variation of the PM gain and unexpected noises, increase probably the error to a conservative 20% at 3 TeV and 15% at 20 TeV.

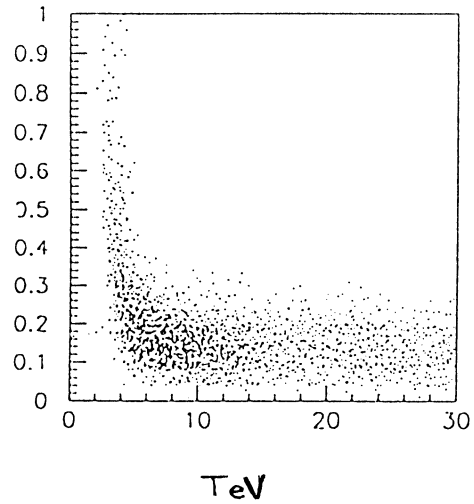


Fig. 7. Calculated $\Delta E/E$ as a function of reconstructed energy.

For gammas the hadronicity is peaked at 1, with a tail extending up to 3.5, Fig 8a. For hadrons, where the azimuthal distribution integrated over the radial distribution is most uneven, the hadronicity distribution is wider, Fig 8b, and matches nearly the experimental one, Fig 8c. The cut in hadronicity at 3.5, while keeping all gammas, will remove part of the hadrons, mostly in the high energy region over 10 TeV.

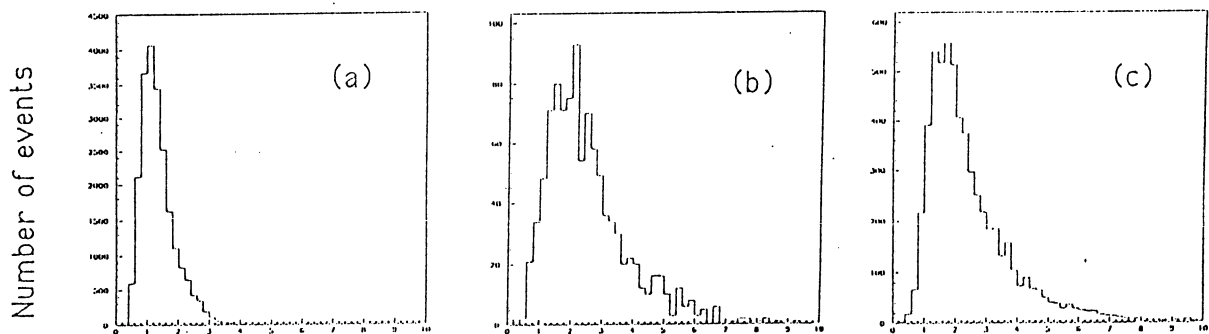


Fig . 8. Distributions of "hadronicity" : a) Monte. Carlo gammas b) M.C. hadrons c) Real events

In the process of energy evaluation we always fitted on all events the radial distributions of M.C. gammas ! Hence the hadrons are evaluated with the wrong energy. In order to approach the real hadron energy by this method we have to scale the reconstructed energy by an average factor of 1.35, moreover slightly dependant of energy. This factor can be obtained using the M.C. generated hadrons.

New developments.

ADC dynamics

Increase of the ADC dynamics, from 1 to 300 ph.el. to 1 to 1200 ph.el. by adding an extra ADC on each telescope. This has already been implemented and used in the 92-93 runs.

Hadron rejection

Two additional telescopes ,19 and 20, of the same size and quality as the others, have been added for test purposes in the middle of the field. They started and will be used to help the discrimination of hadrons from the gammas. They are not used for the cone reconstruction.

Fast pulse shape analysis:

The 19th has been equipped in January 93 with a waveform digitizer Le Croy 6880A , sampling time 0.742 ns, memory depth of 4 μ s . In the first part of the year it was equipped with the same PM (XP 2020) and amplifier than the other 18. The aim was to check if the reproduction of the pulse shape by the M.C. was in agreement with the measurement as a function of the distance to impact.

The full size pulse, as well as an attenuated one by a factor 10 and delayed by 56 ns, Fig 9, are buffered waiting for the main trigger to come and to validate their read out. The pulses are parametrized by their rise time (10-90%), their fall time (10-90%) and their width at respectively 10, 20 and 50% of the full heigth. Results are shown in Fig.10. and show a general agreement with the simulations.

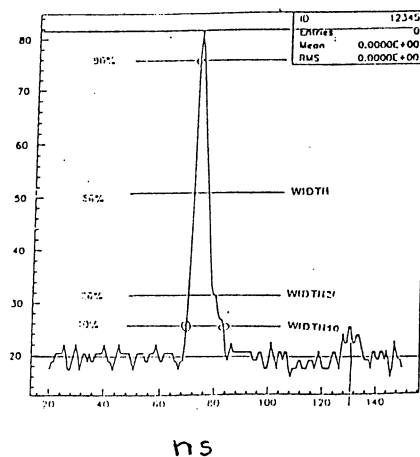


Fig. 9. Output of the waveform analyser. Full size and delayed 1/10 size pulse.

The bandwidth of both the PM and the preamplifier (150 MHz) makes of the pulse shape a poor discriminant of the nature of the incident

particle. In the next runs, starting september 1993, the XP 2020 will be replaced by an Hamamatsu H 2083 of 0.7ns rise time , a fast x 10 preamplifier, 400 MHz bandwidth and a short cable connection. We will then make use of the relation between the pulse shape and the distance to the impact point to discriminate between gamma and hadron showers, mainly on the basis of differences between fall time and widths. The majority of the selected showers falls between 50 and 120 m from the 19th telescope, distances where the pulse shape is the most sensitive to the nature of the initial particle.

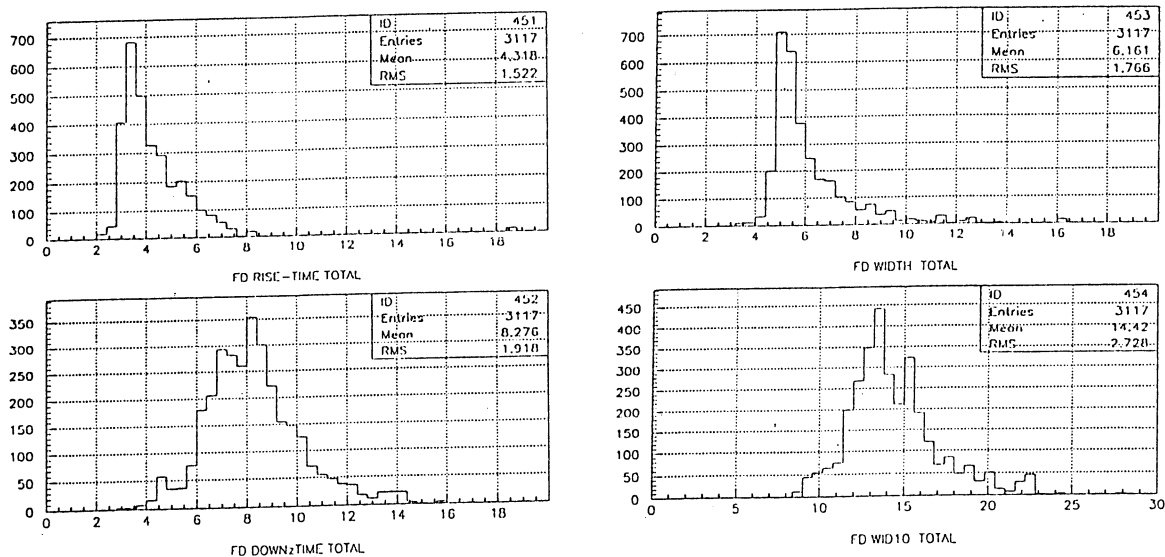


Fig. 10. Pulse size analysis : a) Leading edge b) trailing edge c) Pulse width at 50% height d) Pulse width at 10% height

The rejection may not be very strong for initial protons but increases for nuclei. Although this cut be not independent of other geometrical rejections, an overall factor of 3 may be hoped for.

Imaging .

The 20th telescope has been equipped in may 93 - thanks to the help of the Gran Sasso EAS TOP Collaboration- with an RTC XP 4702 PM of 64 pixels $(2.54 \text{ mm})^2$. The total field covered is $(2.7^\circ)^2$, each pixel covering $(0.33^\circ)^2$.

The geometrical aberration of the mirror is smaller than the pixel size, but at the edge of the field the optical distortion is higher.

At the threshold energy of 3 TeV, the average number of collected photo electron is about 10, which will be shared between 4 pixels for a gamma. The ADC sensivity is 3 channels/ph.el. and the night sky background of 0.1 ph.el./pixel. The PM alignment is checked by imaging of relatively bright stars ($m < 4$), at a 2 mr precision.

The imaging, rather crude at 3 TeV, may become efficient beyond 7 TeV where it is in fact most needed.

The role of the imaging may be efficient at two levels:

- To help to reject the hadrons by the usual methods of core to halo ratio of the image.
- To provide an estimation of the shower position on the field, at least in one direction and thus to introduce one or two extra constraint in the fit of the cone on the apex position. It will be then possible to use events with a smaller number of telescopes hit, at the best 10 instead of 12, and use part of the not contained events, thus extending the effective area of the field.

Altogether we hope a factor 2 in hadron rejection by imaging (here again this rejection will not be independent of the other rejections), and a factor of order 3 in increased number of events using less telescopes in the fit.

Conclusions.

For the next two years THEMISTOCLE intends to take data without major extension of the apparatus, most of the effort of the Collaboration being devoted to the CAT project.

Nevertheless with the effort concentrated on the rejection of hadrons and the data efficiency we could hope to reach a additional factor close to 10 in efficiency for gammas. This will raise the sensitivity of the experiment at the level of

$$N_{\sigma} = 2. \sqrt{\frac{\Phi}{\Phi_{cr}} t}$$

6 s.d. in 10 hours for a Crab like source.

References.

- [1] Gamma ray spectrum of the Crab nebula in the multi-TeV region.
P. Baillon et al. Submitted to Astro-particle Physics